Tropical Journal of Natural Product Research

Original Research Article

Molecular Docking, Molecular Dynamic Simulation and ADME of Some Plant Extracts and their Effects on COVID-19 Patients

Dhia A. Hanoush[1]*, Amjad H. Al-Auqaili[2], Mustafa Mansour[3], Arabinda Ghosh[4]

[1]*Dhi Qar Education Directorate,Dhi Qar, Iraq*
[2]*Iraqi Ministry of Health,Baghdad, Iraq*
[3]*Department of Medicinal Chemistry, Faculty of Pharmacy, Nahda University, Beni Suef, Egypt*
[4]*Microbiology Division, Department of Botany, Gauhati University, Gauhati University, Guwahati, Assam, India*

ARTICLE INFO

ABSTRACT

The coronavirus disease 2019 (COVID-19) is caused by the recently discovered coronavirus and affects several countries worldwide. Some medications may alleviate or minimize some of the disease symptoms, but no drug have been proven to prevent or cure it. However, this study was aimed at investigating the role of some medicinal plants as potent inhibitors of COVID-19 main protease (MPro). More than 250 plant extracts with antiviral activity were exploited for their potential SARS-CoV2 medication using molecular docking. The conformational stability of the compounds extracted from the plants with MPro interactions was evaluated using molecular dynamics simulations. Then, the plant extracts with the highest binding energies were used for treatments by administering them to 50 COVID-19 patients, while the other 50 cases received only the drug without the plant extracts. The results of the theoretical analysis revealed high binding energies for seven compounds. Alliin stabilized COVID-19's MPro while retaining critical connections and remained stable throughout the simulations. Marrubin and thymoquinone are also capable of protein stabilization over the simulated time. The test plants were observed to be effective against the virus in the COVID-19 patients, with a disease symptom improvement response rate of 78-86 and 60-72% for the first and second groups, respectively. Also, the percentage of oxygen increased from the second day after taking the extracts. Ground-glass opacity disappeared from the second group that received the plant extracts. The findings of this study suggest that these compounds have a great potential for therapeutic activity if isolated and administered alone.

Keywords: Alliin, Marrubin, Molecular docking, SARS-CoV2, Thymoquinone, MD simulation

Introduction

Coronavirus is a virus family that can cause disease in both animals and humans. A variety of coronaviruses cause respiratory infections in humans, ranging in severity from ordinary colds to more severe disorders.[1] Coronavirus disease 2019 (COVID-19) is caused by the recently discovered coronavirus in Wuhan, China, in December 2019. The disease has now become a pandemic, affecting several countries worldwide. Some medications may alleviate or minimize some of the symptoms of COVID-19, but no treatments have been proven to prevent or treat this disease. Antibiotics do not eliminate viruses; rather, they treat bacterial infections. Because COVID-19 is caused by a virus, antibiotics are not first choice in treating it. Antibiotics are not recommended for the treatment or prevention of COVID-19. Patients with severe COVID-19 complications may be offered antibiotics to treat or prevent secondary bacterial infections. Since ancient times, medicinal plants have been used as natural remedies for a wide range of ailments, including viral infections,[2] because they contain a variety of compounds that aid in the treatment of a variety of diseases.

*Corresponding author. E mail: Dia.adnan@gmail.com
Tel: 009647737275370

With the spread of media reports about the discovery of "innovative" drugs that could treat people infected with the virus, the World Health Organization rushed to refute such claim on February 6, 2020, stressing that there are no known effective treatments. This opened the door to alternative means of preventing the killer virus. One of these methods is to use medicinal plants with antiviral properties, such as garlic and *Nigella sativa*. These medicinal herbs have the advantage of containing effective anti-viral compounds.

Molecular docking is a method for predicting the preferred binding location of one molecule, known as a ligand, to a second, known as a receptor.[3] Receptors are 3D protein structures that are usually published in the protein data bank. When the 3D structure of the test protein is not available, homology modeling is used instead. Docking is a computational method that has become a popular drug discovery tool, particularly in academic settings, due to its low cost and perceived ease of use.[4,5] The first crucial component of molecular techniques is the searching algorithm, and the second is the scoring function. These two components collaborate to identify the most stable binding conformation between the two partners. The searching algorithm component is in charge of exploring the searching space by making systematic adjustments to the orientation and conformation of the molecule.[6] Many searching algorithms have been developed to look for a more stable compound between the two partners within the conformational space. The scoring function, on the other hand, evaluates or, as the name implies, scores the ligand conformations generated by the search method. The searching function may appear overwhelming at first glance, but it is only the sum of the basic bonding and non-bonding characteristics of the two molecules that comprise the complex. It is necessary to be familiar with the scoring

functions of the docking software used to understand and analyze the obtained results.

Most scoring functions are conceptually similar but have varying degrees of simplification, as well as differences in the molecular mechanism and force field used to estimate the energy of the pose within the binding site. Complexes computed using molecular docking techniques can be more or less stable based on a variety of parameters, but the binding affinity determined with the scoring function can be an accurate predictor of binding strength.[7,8] A high negative volume of stability usually suggests that the examined ligand and the receptor have high binding energy. On the other hand, a positive value would indicate a significant collision or repulsion between the atoms of the participating molecules in the docking experiment. Doubtful docking algorithms with a positive scoring value, however, are rather resilient in this regard, and they will eliminate any unrealistic poses from the final list of ligand solutions. So, after estimating the binding position between the ligand and the receptor, the major goal is to analyze the interaction between the molecules at an atomic level, and docking approaches enable the screening of entire libraries in this manner. The input structure must be in a stable state; it must be at an energetic minimum. It should be noted that docking approaches require two types of input structures: ligands on the one hand and proteins on the other. In the case of ligands, semi-empirical or quantum chemical optimization approaches can be employed, which are implemented in a variety of software packages like mopac, gamus, or Gaussian.[9–11]

The coronavirus (SARS-CoV-2) main protease (Mpro) is a protease that participates in viral replication by cleaving the polyprotein. Mpro is divided into three domains and functions as a homodimer.[12] Chain A represents a 3C-like proteinase co-crystallized with the selective inhibitor N3 in the crystal structure of COVID-19 main protease in complex with an inhibitor N3 (PDB ID: 6LU7). To achieve a good *in vivo* response, pharmacokinetic and pharmacodynamic aspects must be balanced.[12] Christopher A. Lipinski, a medicinal chemist, studied the physicochemical properties of over 2,000 drugs and came up with five criteria for drug-likeness: molecular weight should be less than 500, logP ≤ 5, hydrogen bond donors (HBDs) ≤ 5, and hydrogen bond acceptors (HBAs) ≤ 10. Drug-like candidates are often favored to follow the "rule of five," with a special emphasis on lipophilicity. Poor passive absorption or permeability of a chemical is more likely if it violates two or more criteria.[13] PSA is defined as the sum of the surfaces of polar atoms (often oxygen, nitrogen, and connected hydrogen) in a molecule. It is an important factor in human intestinal absorption, cell permeability, and blood-brain barrier (BBB) penetration. For compounds to be absorbed through the intestine, they should be less than 140 Å2 and less than 90 Å2 to penetrate the BBB. PSA is also involved in the calculation of percentage absorption (%ABS) as it is inversely proportional to %ABS.[14,15]

%ABS = 109 − 0.345 PSA

The present study was conducted to investigate the function of some medicinal plants as a powerful inhibitor of COVID-19 major protease.

Materials and Methods

Resource materials
Molecular docking studies were carried out using MOE vs 2015.10. Nanoscale molecular dynamics was carried out using Desmond version 2020.1. The structural formula of the active constituent was taken from the drug bank, and some of them were painted in professional ChemDraw 19.0.0.22, and others were downloaded from the PubChem website (https://pubchem.ncbi.nlm.nih.gov) in SDF format since there was more than one active compound in each plant. Two hundred and fifty (250) active compounds were tested, and molecular docking was performed.

Molecular docking
To ensure the validity of the docking protocol, the co-crystallized native ligand was re-docked into the active site. The coordinates of the best scoring docking pose of the native ligand were compared with its coordinates in the co-crystallized PDB file based on the binding mode and root mean square deviation (RMSD). The re-docked ligand had an RMSD of 2.4837 between the docked pose and the co-crystallized ligand (energy score (S) = -9.6897 kcal/mol). According to recent

studies, the active site of this protein contains Glu166, which is the most repeated and appears to be the most significant, Gln189, His41, Cys145, and Thr190. (16–18).

Molecular dynamic simulation
According to binding energy, the compounds alliin, thymoquinone and marrubin showed the best affinity for SARS-CoV2 main protease. As a result, molecular dynamics (MD) simulations were used to assess the conformational stability of alliin, thymoquinone, and marrubin with major protease interactions.[19] The MD simulation was carried out to analyze the stability of alliin, thymoquinone, marrubin, and the SARS-CoV2 main protease (PDB ID: 6LU7) complex for 100 ns using the Desmond 2020.1 from Schrödinger, LLC. The OPLS-2005 force field,[20–22,] and explicit solvent model with the SPC water molecules were used in this system with a periodic boundary condition in an orthorhombic box and having dimensions 10Å x 10Å x 10Å.[23] Sodium ions (Na^+) were added to neutralize the charge. Furthermore, a 0.15 M NaCl solution was added to the system to simulate the physiological environment. To retrain over the protein-Aptamer complex, the system was first equilibrated using an NVT ensemble for 100 ps. Followed by this a short run equilibration and minimization using an NPT ensemble for 12 ps was applied. The NPT ensemble was set up using the Nose-Hoover chain coupling scheme,[24] with a temperature of 300 K, a relaxation time of 1.0 ps, and a pressure of 1 bar maintained throughout the simulations. A time interval of 2 fs was used. Pressure was controlled using the Martyna-Tuckerman-Klein chain coupling scheme,[25] barostat method, and a relaxation time of 2 ps. For long-range electrostatic interactions, the particle mesh Ewald technique,[26] was employed, and the radius for coulomb interactions was set to 9Å. RESPA integrator was used to calculate the non-bonded forces. The RMSD, root mean square fluctuation (RMSF), of C-α backbone of the protein, and number of H-bonds formed between alliin, thymoquinone, and marrubin and S SARS-CoV2 main protease, were employed to monitor the stability of the MD simulations.

Study groups and administration of plant extract
The plants were evaluated on 100 COVID-19 patients. One hundred COVID-19 patients ((age ranged from 30 to 40 years) receiving treatment in Private clinic at Corona treatment center / Qalat Suqar Hospital in Qalat Suqar, Thi Qar / Iraq. They were divided into two groups. The first control group followed the Iraqi Ministry of Health's treatment protocol, which included: Immune booster cap (1*1), Zocin or ceftriaxone vial (1g drip), and Doliprane tab (1000 mg 1*2). The second group (the experimental group) followed the same procedure but also consumed a teaspoon of black seed twice daily and a clove of garlic three times daily.

Results and Discussion

Predicted pharmacokinetic parameters
As mentioned in tables 1 and 2, except for rutin, all investigated compounds obeyed Lipinski's rule of five, which is considered an important parameter for selecting drug-like candidates based on previous calculations and observations. Rutin did not obey Lipinski's rule since it has a larger molecular weight of 610.52, an H-bond donor of 10, and an H-bond acceptor of 16, making it unsuitable for oral absorption. Other compounds had molecular weights of less than 500, logP values of less than 5, a low number of H-bond donors, a low number of H-bond acceptors, and a low number of rotatable bonds, indicating adequate oral bioavailability. Alliin, marrubin, and thymoquinone, on the other hand, displayed high %ABS ranging from 81.26 to 97.22%, showing that they are potent oral absorbable agents.

The outcome of the molecular docking procedure
According to recent research, the active site of SARS-CoV-2 Mpro contains Glu166, which is the most repeated and appears to be the most important, as well as Gln189, His41, Cys145, and Thr190. The seven compounds were docked into the active site of COVID-19 primary protease in conjunction with an inhibitor N3 (PDB ID: 6LU7), utilizing the Molecular Operating Environment (MOE 2020.0101) developed by the Chemical Computing Group. Fifty postures from each compound were scored using the initial rescoring

approach (London dG) and the final re-scoring methodology (London dG) after placement using Triangular Matcher and post-placement refining using Force Field. The docking procedure results are shown in Tables 3 and 4. The docking score (affinity Kcal/mol), distances (Å) from the main residues, a functional group involved in the interaction, and type of interaction were all taken into account. All the figures in Table 3 and Figure 1 were generated using the Discovery Studio 2021 Client Visualizer. In decreasing order, all identified compounds demonstrated moderate to good affinity to the active site of COVID-19 major protease, particularly rutin, alliin, thymoquinone, and marrubin. The four compounds have strong interactions with key amino acids required for the inhibition of Mpro of COVID-19, such as Cys145, Glu166, and Gln189, making them effective inhibitors of this enzyme and candidates for overcoming COVID-19 infections.

The outcome of the molecular dynamic simulations
The MD simulations of alliin-, thymoquinone-, and marrubin-bound SARS-CoV2 main protease are displayed in Figure 2. With 0.7 Å deviation, the RMSD of 100 ns MD simulation trajectories revealed the most stable conformation of an alliin-bound major protease protein complex (Figure 2A; red). Meanwhile, the RMSD displacement of the thymoquinone-bound complex was 1.7 Å (Figure 2A; black), and the marrubin-bound complex was 1.8 Å (Figure 2A; green). However, the main protease (apo) without ligand had an RMSD deviation of 2.1 Å (Figure 2A; cyan). The RMSD plots represent the stable conformation of the ligand-bound complex with the major protease, with the alliin-bound complex achieving the best conformation. Figure 2B depicts the root mean square variation (RMSV) of the amino acid residue position of 100 ns simulation trajectories of alliin-, thymoquinone-, and marrubin-bound primary protease. The primary protease linked to alliin has the least amount of amino acid residue variation (Figure 2B, black). Maximum changes were detected at residue positions 360 and 475, ranging between 3-4 Å. The RMSF of the amino acid residue position of 100 ns simulation trajectories of alliin-, thymoquinone-, and marrubin-bound main protease is displayed in Figure 2B. The primary protease linked to alliin has the least fluctuation of amino acid residue variation (Figure 2B; black). Maximum fluctuations were detected at residue positions 360 and 475, ranging between 3-4 Å.

In contrast, thymoquinone-bound main protease showed fluctuations at the residue positions 360, 475, and 510 (Figure 2B, cyan), and high fluctuations were observed in marrubin-bound main protease at the residue positions 430, 455, 505, and 506 (Figure 2B; red). However, the apo-protease displayed the highest fluctuations, suggesting that alliin-bound primary protease has the best stability. The formation of H-bonds is an important aspect in demonstrating the protein and ligand interaction during a 100-ns simulation. As observed in Figure 2C, allin forms an average of 5 H-bonds with the major protease of SARS-CoV2 during the simulation. Thymoquinone (Figure 2D) and marrubin (Figure 2E) were 4 and 2, respectively. In comparison to thymoquinone and marrubin, the pattern of H-bond formation indicates that alliin has a more stable interaction with the main protease.

*Effect of test plants on patients with COVID-19*
The experimental results of the two groups that received the proposed treatment revealed a significant disparity. The cure rate for the first group (experimental), which received garlic and nigella seed treatments with a response period of 3-6 days, was between 78 and 88%. It is worth noting that the percentage of oxygen increased after only 24 hours of taking the garlic and black seed treatment, reaching 97% with no other treatment. Patients were not given anticoagulants during their treatment.

Table 1: *In silico* physicochemical properties of the compounds as determined by Molinspiration.

Compound	LogP[a]	M. Wt[b]	HBA[c]	HBD[d]	Lipiniski's Violations	NORTB[e]	TPSA[f] Å²	%ABS[g]
Alliin	- 3.39	177.22	4	3	0	5	80.39	81.26
Carnosol	4.61	330.42	4	2	0	1	66.76	85.96
Choline	-4.24	104.17	2	1	0	2	20.23	102.02
Diterpene	4.23	320.47	3	1	0	5	54.37	90.24
Marrubin	2.70	398.38	8	3	0	3	59.67	88.41
Rutin	-1.06	610.52	16	10	3	6	269.43	16.04
Thymoquinone	1.90	164.20	2	0	0	1	34.14	97.22

[a]LogP: Logarithm of compound partition coefficient between n-octanol and water; [b]M.Wt; Molecular weight; [c]HBA: Number of hydrogen bond acceptors; [d]HBD: Number of hydrogen bond donors; [e]NROTB: Number of rotatable bonds; [f]TPSA: Topological polar surface area; [g]%ABS: Percentage of absorption.

Table 2: Phytochemicals with their sources, structures and Lipinski's rule.

Compound	Vegetarian source	Structure	M.W.	Lipinski's rule
Alanine	Garlic		177.22	yes
Marrubiin	Hyssop		332.44	yes
Choline	Dandelion		104.17	yes
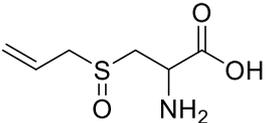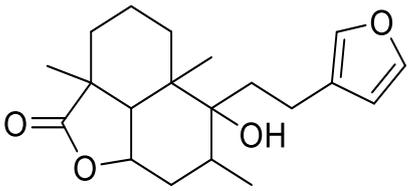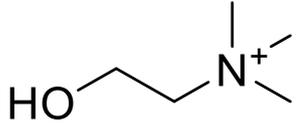
| Diterpene	Hyssop Diterpene deriv		320.47	yes
Rutin (quercetin-3-rutnoside)	Sambucus nigra		610.52	No
Carnsol	Rosemary		330.42	yes
Thymoquinone	*Nigella sativa*		164.20	yes
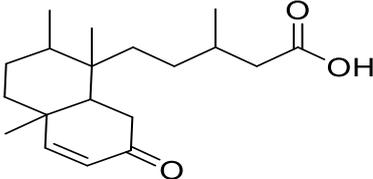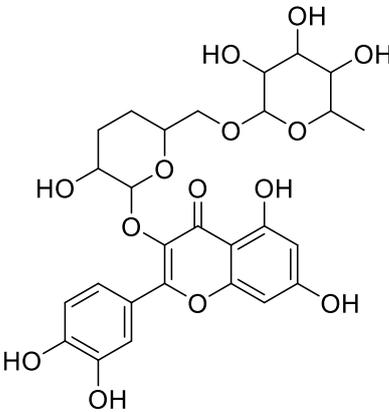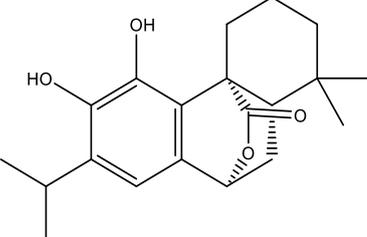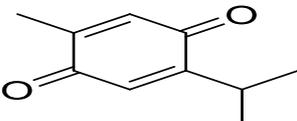
Table 3: Molecular docking results for seven compounds at the active site of COVID-19 main protease (PDB ID: 6LU7).

Compound	The crystal structure of COVID-19 main protease in complex with an inhibitor N3 (PDB ID: 6LU7)				
	Affinity Kcal/mol	Distance (in Å) from main residue		Interaction	2D Figures
Alliin	-9.6962	4.98	Cys145	Hydrophobic	
		1.95	Glu166	H-Donor	
		2.68	Gln189	H-Acceptor	
		2.41	Thr190	H-Donor	
Carnosol	-6.3362	3.40	Cys145	H-Acceptor	
		3.05	Glu166	H-Donor	
		4.81	His41	Hydrophobic	
		2.62	Met165	H-Acceptor	
		5.39	Met49	Hydrophobic	
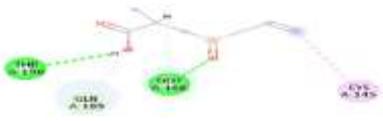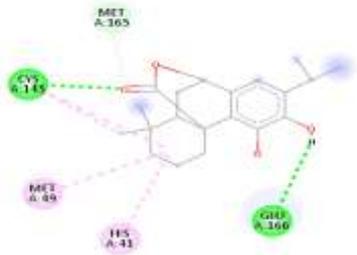
Choline	-5.3932	4.44	His41	Pi-Orbitals
		2.83	Asp187	H-Acceptor
		2.98	His164	H-Donor
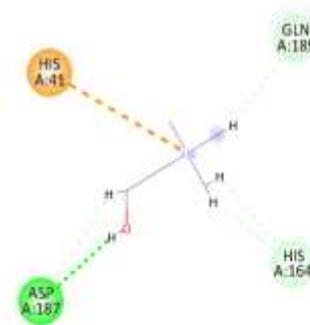
Diterpene	-7.8537	2.39	Glu166	H-Donor
		2.98	His163	H-Acceptor
		2.38	Phe140	H-Acceptor
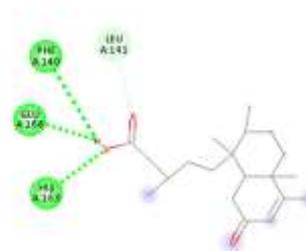
Marrubin	-8.5204	4.99	Cys145	Hydrophobic
		2.15	Glu166	H-Donor
		1.65	Gln189	H-Acceptor
		1.96	His163	H-Acceptor
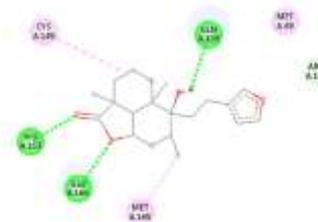
Rutin	-15.0798	3.14	Cys145	H-Acceptor
		2.44	His41	H-Acceptor
		4.94	Glu166	H-Donor
		2.48	Phe140	H-Acceptor
		2.36	His164	H-Donor
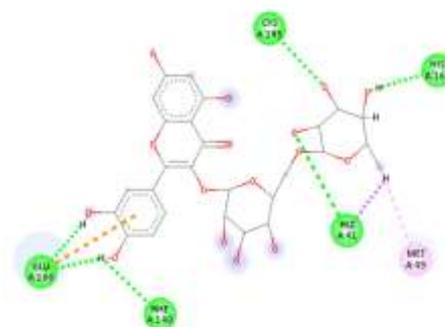
Thymoquinone	-9.0042	3.35	Cys145	H-Acceptor
		2.11	Glu166	H-Acceptor
		2.34	His41	H-Acceptor
		4.57	Met49	Hydrophobic
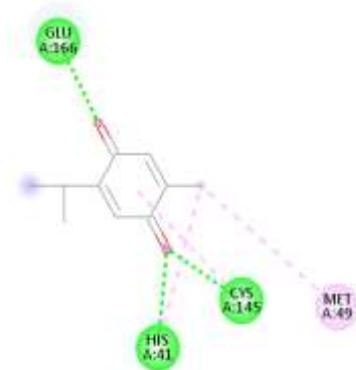
Table 4: Disease symptoms and percentages of response for each group.

Symptom	Abdominal pain and hemoptys	Pharyngeal pain	Slenderness and Loss of appetite	Dyspnea	Stomachache and Diarrhea	Dry cough	Loss of smell	Fever and Sweating at night
Percentage of response for testing group	87-86%	83%	84%	84%	84%	88%	85%	86%
Percentage of response for controlling group	60-65%	64%	66%	69%	70%	72%	71	71
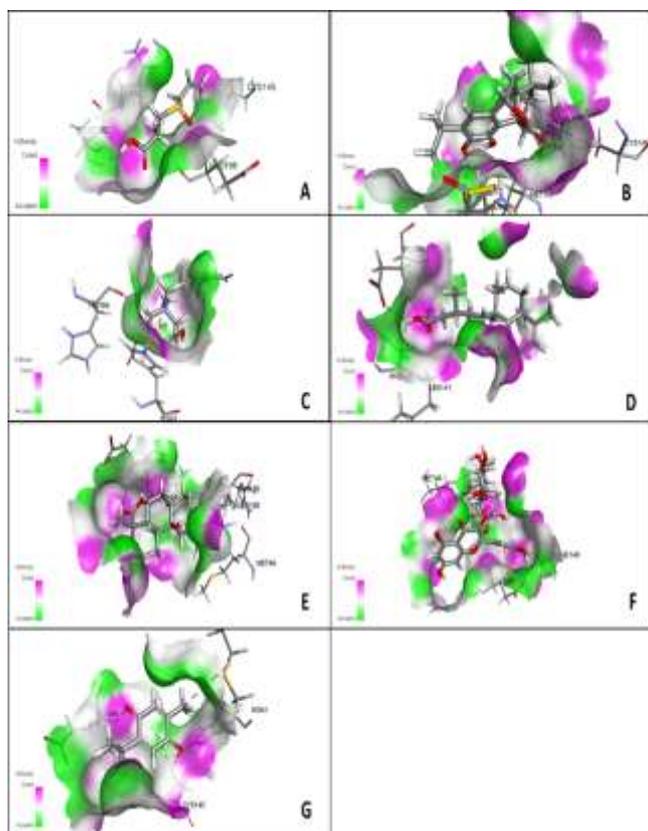
Figure 1: 3D structure of molecular docking results for the compounds at the active site of COVID-19 main protease (PDB ID: 6LU7). A: Alliin; B: Carnosol; C: Choline; D: Diterpene; E: Marrubin; F: Rutin; G: Thymoquinone.
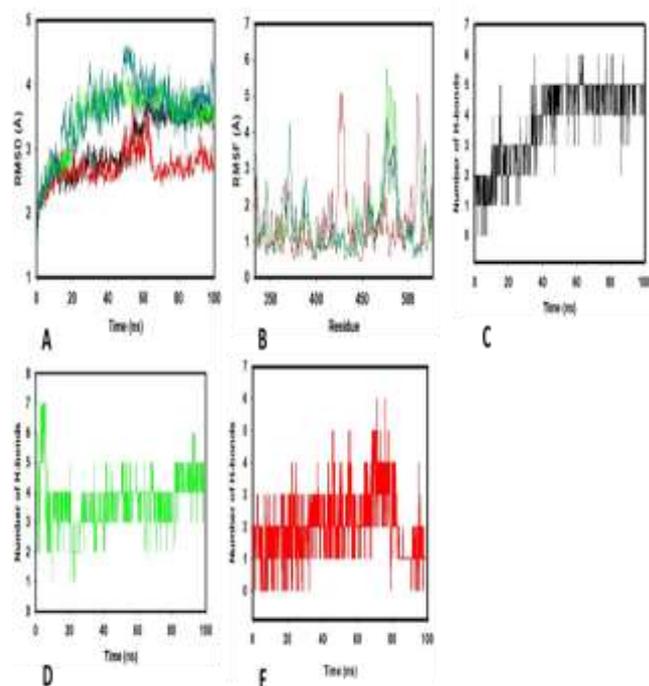
Figure 2: Analysis of MD simulation trajectories of 100 ns. A: RMSD plots of Alliin, Thymoquinone and Marrubin bound SARS-COV2 main protease; B: RMSF plots of Alliin, Thymoquinone and Marrubin bound SARS-COV2 main protease, Number of hydrogen bonds formed with; C: Alliin; D: Thymoquinone; E: Marrubin bound to main protease.
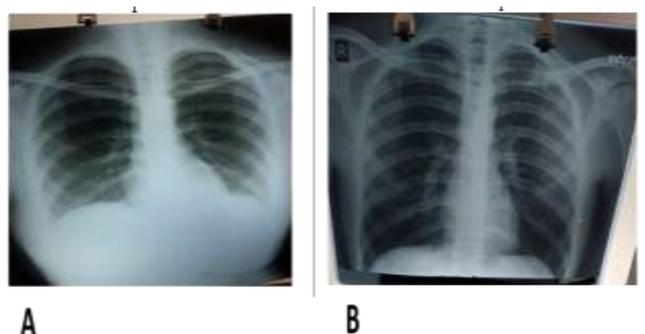
Figure 3: Chest X-ray of COVID-19-infected patient. A: Before treatment with plant extract; B: After treatment with plant extract

The first group (the control group), as shown in Table 4, was not administered to the test plants; the cure rate for symptoms ranged from 60 to 72%. It was observed that the reaction rates for respiratory symptoms ranged between 83 and 84%. This is a higher rate than the control group, which had a response rate of 70%. When it comes to gastrointestinal issues, the reaction rate of 84-87% is very high when compared to the response rate of the control group, which was 60-70%.

The chest X-ray (radiograph) for the two groups revealed that ground-glass opacity (GGO) disappeared from the second group that received the plant extracts. GGO is an area in the chest X-ray that appears grey or hazy due to the displacement of air by fluids. This sign was visible in those infected with the COVID-19 virus, but it was missing in the majority of patients in the second group that received the test plants (Figure 3). It should be noted that the doses were consumed as a whole plant comprising more than one plant extract, which may affect the other. If the extracts are administered individually, the experimental effect may be better and the response rate may have been higher due to their strong affinity for the virus.

Conclusion

This study aimed to discover the antiviral effect of the studied plant extracts (Alliin, Carnosol, Choline, Diterpene, Marrubin, Rutin, Thymoquinone), and their ability to treat the covid-19 infection.
The results of the theoretical analysis revealed high binding energies for the seven compounds and remained stable throughout the simulations. These research results indicated the ability of the use of these extracts as active drug against covid-19 virus.

Conflict of Interest

The authors declare no conflict of interest.

Authors' Declaration

The authors hereby declare that the work presented in this article is original and that any liability for claims relating to the content of this article will be borne by them.

References

1. Abebe EC, Dejenie TA, Shiferaw MY, Malik T. The newly emerged COVID-19 disease: A systemic review. Virol J Biomed Central. 2020; 17:96.
2. Lazzarotto-Figueiró J, Capelezzo AP, Schindler MSZ, Fossá JFC, Albeny-Simões D, Zanatta L, et al. Antioxidant activity, antibacterial and inhibitory effects of intestinal disaccharidases of extracts obtained from *Eugenia uniflora* l. seeds. Braz J Biol. 2021; 81(2):291–300.
3. Wang YJ, Wang L, Bao L. Exploring the active compounds of traditional Mongolian medicine in the intervention of novel coronavirus (COVID-19) based on molecular docking method. J Funct Foods. 2020; 1:71.
4. Arunkumar B, Fernandez A, Laila SP, Nair AS. Molecular docking study of acyclovir and its derivatives as potent inhibitors in novel COVID-19. Int J Pharm Sci Res. 2020; 11(9): 4700-4705.
5. Fischer A, Smieško M, Sellner M, Lill MA. Decision making in structure-based drug discovery: Visual inspection of docking results. J Med Chem. 2021; 64:2489–2500.
6. Mohammad T, Mathur Y, Hassan MI. InstaDock: A single-click graphical user interface for molecular docking-based virtual high-throughput screening. Brief Bioinform. 2021; 22(4): bbaa279. doi: 10.1093/bib/bbaa279. PMID: 33105480.
7. Thapa B and Raghavachari K. Energy decomposition analysis of protein-ligand interactions using the molecules-in-molecules fragmentation-based method. J Chem Inf Model. 2019; 59(8):3474–3484.
8. Riza YM, Parves MR, Tithi FA, Alam S. Quantum chemical calculation and binding modes of H1R; a combined study of molecular docking and DFT for suggesting therapeutically potent H1R antagonist. Silico Pharmacol. 2019; 7(1): 1. doi: 10.1007/s40203-019-0050-3. PMID: 30863716; PMCID: PMC6389732
9. Gamus A and Chodick G. Telemedicine after COVID-19: The Israeli perspective. Isr Med Assoc J. 2020; 22(8):467–469.
10. Maia JDC, Urquiza-Carvalho GA, Mangueira CP, Santana SR, Cabral LAF, Rocha GB. GPU linear algebra libraries and GPGPU programming for accelerating MOPAC semiempirical quantum chemistry calculations. J Chem Theory Comput. 2012; 8(9):3072–3081.
11. Wilson JT, Borovitskiy V, Terenin A, Mostowsky P, Deisenroth MP. Pathwise conditioning of gaussian processes. J Mach Learn Res. 2021; 22: 7470–7480.
12. Ekins S, Mottin M, Ramos PR, Sousa BK, Neves BJ, Foil DH, Zorn K, Braga R, Coffee M, Southan C, Puhl A, Andrade C. Déjà vu: Stimulating open drug discovery for SARS-CoV-2. Drug Discov Today. 2020; 25:928-941.
13. Grime KH, Barton P, McGinnity DF. Application of *in silico*, *in vitro* and preclinical pharmacokinetic data for the effective and efficient prediction of human pharmacokinetics. Mol Pharm. 2013; 10(4):1191–1206.
14. Alegaon SG, Alagawadi KR, Sonkusare PV, Chaudhary SM, Dadwe DH, Shah AS. Novel imidazo [2, 1-b][1, 3, 4] thiadiazole carrying rhodanine-3-acetic acid as potential antitubercular agents. Bioorg Med Chem Lett. 2012; 22(5):1917–1921.
15. Amin NH, El-Saadi MT, Ibrahim AA, Abdel-Rahman HM. Design, synthesis and mechanistic study of new 1, 2, 4-triazole derivatives as antimicrobial agents. Bioorg Chem. 2021; 111:10484.
16. Yan Y, Shen X, Cao Y, Zhang J, Wang Y, Cheng Y. Discovery of anti-2019-nCoV agents from 38 Chinese patent drugs toward respiratory diseases via docking screening.Preprints2020,2020020254(doi: 10.20944/preprints202002.0254.v2).
17. Khaerunnisa S, Kurniawan H, Awaluddin R, Suhartati S, Soetjipto S. Potential inhibitor of COVID-19 main protease (Mpro) from several medicinal plant compounds by molecular docking study: *Preprints* 2020, 2020030226 (doi: 10.20944/preprints202003.0226.v1).
18. Sayed AM, Khattab AR, AboulMagd AM, Hassan HM, Rateb ME., Zaid H, Abdelmohsen UR. Nature as a treasure trove of potential anti-SARS-CoV drug leads: a structural/mechanistic rationale. RSC Adv. 2020; 10(34):19790–19802.
19. Mansour MA, Aboul-Magd AM, Abdel-Rahman HM. Quinazoline-Schiff base conjugates: *in silico* study and

ADMET predictions as multi-target inhibitors of coronavirus (SARS-CoV-2) proteins. RSC Adv. 2020; 10(56):34033–34045.

20. Bowers KJ, Chow E, Xu H, Dror RO, Eastwood MP, Gregersen BA, Klepeis J, Kolossvary I, Moraes M, Sacerdoti F, Salmon J, Shan Y, Shaw D. Scalable algorithms for molecular dynamics simulations on commodity clusters. In: Proceedings of the 2006 ACM/IEEE Conference on Supercomputing, SC'06. 2006. 43–43 p.

21. Chow E, Rendleman CA, Bowers KJ, Dror RO, H D, Gullingsrud J, Sacerdoti F, Shaw D. Desmond performance on a cluster of multicore processors. Simulation. 2008; *DE Shaw Research Technical Report DESRES/TR--2008-01*.

22. Shivakumar D, Williams J, Wu Y, Damm W, Shelley J, Sherman W. Prediction of absolute solvation free energies using molecular dynamics free energy perturbation and the opls force field. J Chem Theory Comput. 2010; 6: 1509–1519.

23. Jorgensen WL, Maxwell DS, Tirado-Rives J. Development and testing of the OPLS all-atom force field on conformational energetics and properties of organic liquids. J Am Chem Soc. 1996; 118:11225–11236.

24. Martyna GJ, Klein ML, Tuckerman M. Nosé–Hoover chains: The canonical ensemble via continuous dynamics. J Chem Phys. 97:2635–2643.

25. Martyna GJ, Tobias DJ, Klein ML. Constant pressure molecular dynamics algorithms. J Chem Physics. 1994; 101:4177–4189.

26. Toukmaji AY and Board JA. Ewald summation techniques in perspective: a survey. Comp Physics Comm. 1996; 95:20-73-92.